Plectasin, a fungal defensin, targets the bacterial cell wall precursor Lipid II

Metazoan and fungal host defence peptides act as specific inhibitors of bacterial peptidoglycan biosynthesis

Tanja Schneider[1], Thomas Kruse[5], Reinhard Wimmer[3], Imke Wiedemann[1], Vera Sass[1], Ulrike Pag[1], Andrea Jansen[1], Allan K Nielsen[2], Per H Mygind[2], Dorotea S Raventós[2], Søren Neve[2], Birthe Ravn[2], Alexandre MJJ Bonvin[4], Leonardo De Maria[2], Anders S Andersen[2,5], Lora K Gammelgaard[2], Hans-Georg Sahl[1] & Hans-Henrik Kristensen[2*]

[1]*Institute for Medical Microbiology, Immunology and Parasitology – Pharmaceutical Microbiology Section, University of Bonn, D-53115 Bonn, Germany*

[2]*Novozymes AS, DK-2880 Bagsvaerd, Denmark*

[3]*Department of Biotechnology, Chemistry and Environmental Engineering, Aalborg University, DK-9000 Aalborg, Denmark*

[4]*Department of Chemistry, Faculty of Science, Utrecht University, 3584 CH Utrecht, the Netherlands*

[5]*Statens Serum Institut, 2300 Copenhagen S, Denmark*

**To whom correspondence should be addressed: hahk@novozymes.com (HHK)*

Host defence peptides such as defensins are components of innate immunity and have retained antibiotic activity throughout evolution. Their activity is thought to be due to amphipathic structures which enable binding and disruption of microbial cytoplasmic membranes. Contrary to this, we show here that plectasin, a fungal defensin, acts by directly binding the bacterial cell wall precursor Lipid II. A wide range of genetic and biochemical approaches identify cell wall biosynthesis as the pathway targeted by plectasin. In vitro assays for cell wall synthesis identified Lipid II as the specific cellular target. Consistently, binding studies confirmed the formation of an equimolar stoichiometric complex between Lipid II and plectasin. Furthermore, key residues in plectasin involved in complex formation were identified using NMR spectroscopy and computational modelling.

Plectasin is a 40 amino acid residue fungal defensin produced by the saprophytic ascomycete *Pseudoplectania nigrella* (*1*). Plectasin shares primary structural features with defensins from spiders, scorpions, dragonflies and mussels and folds into a cystine-stabilized alpha-beta-structure (CSαβ). *In vitro* and in animal models of infection, plectasin is potently active against drug-resistant gram-positive bacteria such as streptococci, while the antibacterial spectrum of an improved derivative, NZ2114 (*2*), also includes staphylococci such as methicillin-resistant *Staphylococcus aureus* (MRSA).

Here we set out to determine the molecular target and specific mechanism by which plectasin kills bacteria. While many host defence peptides (HDPs) act on and disintegrate the bacterial membrane several observations suggested that this is not the case for plectasin.

Growth kinetic measurements of the gram-positive bacterium *Bacillus subtilis* exposed to plectasin clearly demonstrated that plectasin exhibited kinetic behaviour similar to cell wall-interfering agents (*e.g.* vancomycin, penicillin and bacitracin) and not to the rapidly-lytic membrane-active agents (*e.g.* polymyxin and novispirin) or non-lytic antibiotics with replication (ciprofloxacin), transcription (rifampicin) or protein translation (kanamycin, tetracycline) as their primary target (Fig. 1A). Consistent with this, killing kinetics indicated that over a period of approximately one generation time (0.5 hours), treated cells were unable to multiply, but remained viable (Fig. 1B insert), before the number of colony-forming units decreased (Fig. 1B). Next, the effect of plectasin on macromolecular biosynthesis pathways was investigated. The incorporation of radiolabelled isoleucine into protein and of thymidine into nucleic acids was not affected whereas glucosamine, an essential precursor of bacterial peptidoglycan, was no longer incorporated (Fig. 1C). Finally, treatment of *B. subtilis* with plectasin induced severe cell shape deformations as visualized by phase contrast microscopy (Fig. S1). These characteristics are all typical for compounds interfering with cell-wall biosynthesis rather than for membrane disintegration (*3, 4*). Consistently, neither pore formation as measured by K^+ efflux (Fig. 1E) nor changes in membrane potential using TPP^+ or $DiBAC_4$ (Fig. S2AB), nor carboxy-fluorescein efflux from liposomes were detected (Fig. S2C). Thus, despite its amphipathic nature, plectasin does not compromise membrane integrity reducing the risk of unspecific toxicity.

We obtained further support for the cell-wall interfering activity using DNA microarrays to compare the transcriptional responses of plectasin-treated cells with response patterns obtained for a range of reference antibiotics. For both *B. subtilis* 168 and *S. aureus* SG511, we found that the transcriptional profiles overlapped those of established cell wall

biosynthesis inhibitors such as vancomycin and bacitracin (*5, 6, 7, 8*) (Fig. S3; Tables S1 and S2).

The biosynthesis of bacterial cell walls requires a number of steps (*9*). Initially the N-acetylmuramic acid-pentapeptide (MurNAc-pentapeptide), a major constituent of the cell wall building block is produced in the cytoplasm as an UDP-activated precursor before it is transferred onto a membrane carrier, bactoprenolphosphate (reaction I, Fig 2B). The resulting membrane-anchored precursor Lipid I is then further modified to the structural cell wall subunit, Lipid II (reaction II). In some gram-positive bacteria, Lipid II (Fig. 2A) is further decorated by an interpeptide bridge (a pentaglycine peptide in case of *S. aureus* (*10*), reaction III), before it gets translocated across the cytoplasmic membrane to the outside, where it is incorporated into the peptidoglycan polymer through the activity of transglycosylases and transpeptidases (reactions IV). We analysed the intracellular pool of cell wall precursors by reverse HPLC and mass spectrometry and found accumulation of the soluble molecule, UDP-MurNAc-pentapeptide in plectasin-treated cells (Fig. 1D), suggesting that one of the later, membrane-associated or extracellular processes may be targeted by plectasin.

We then analysed the effect of plectasin on the membrane-bound steps of cell wall biosynthesis *in vitro.* Cytoplasmic membranes with associated CW biosynthesis apparatus were isolated and incubated with plectasin and radiolabelled substrates necessary for Lipid II formation. Using thin layer chromatography and subsequent scintillation counting we found the overall synthesis reaction to be strongly inhibited (Fig. 2C). For a more detailed analysis, we cloned the individual CW biosynthesis genes from *S. aureus*, expressed them in *Escherichia coli* and analysed the activity of the purified enzymes in the presence of plectasin by measuring the amount of product formed. These enzymes included MraY (Fig. 2B, reaction I); MurG (Fig. 2B, reaction II); FemXAB (Fig. 2B, reaction III); and PBP2 (Fig. 2B, reaction IV). Whereas the MraY reaction was not affected by plectasin, we found the MurG, FemX and PBP2 reactions to be inhibited in a dose-dependent fashion (Fig.2C). For these three enzymes, Lipid I (MurG) or Lipid II (FemX and PBP2) are substrates and significant inhibition of the reactions was only observed when plectasin was added in equimolar concentrations with respect to Lipid I or Lipid II (Fig. 2C). Thus plectasin, similar to glycopeptide antibiotics (*e.g.* vancomycin (*11, 12*)) and lantibiotics (*13, 14*), may form a stoichiometric complex with the substrate rather than inhibiting the enzyme. To further validate this we incubated either Lipid I or II with plectasin in various molar ratios and used thin layer chromatography to analyse the migration behaviour. Free Lipid I and II as well as free peptide were found to migrate to defined positions in the chromatogram, while the Lipid

I/II-plectasin complex remained at the start point (Fig. 2D). Only at an equimolar ratio, was neither free Lipid I/II nor free peptide detectable, indicating the formation of a 1:1 stoichiometric complex.

We further analysed the interaction of both Lipid I and II with plectasin using a liposome system with membranes composed of phosphatidylcholine and Lipid II (0.2 or 0.5 mol%) and ^{14}C-labelled plectasin. We found the maximum number of plectasin molecules that bound to liposomes to approximately match the number of Lipid II molecules available on the liposome surface (Fig. S4). Using Scatchard plot analysis, we determined an equilibrium binding constant of $1.8x10^{-7}$ mol for Lipid II and $1.1x10^{-6}$ mol for Lipid I, suggesting that the second sugar in Lipid II, the N-acetyl glucosamine contributes to the stability of the complex.

To gain further insight into the structural nature of the plectasin/Lipid II interaction at the membrane interface we measured chemical shifts changes for ^{15}N-labelled plectasin. Heteronuclear single quantum coherence (HSQC) nuclear magnetic resonance (NMR) spectra were measured either in solution or upon binding membrane-mimicking dodecylphosphocholine (DPC) micelles (Fig. S5, Fig. S6). Fitting the binding data to a Langmuir isotherm yielded a free enthalpy of binding ΔG=-27±1 kJ/mol (Fig. S7). Backbone H^N and N atoms of ten residues (G6, W8, D9, A31, K32, G33, G34, F35, V36 and C37), which in the tertiary structure all locate to one end of plectasin, exhibited marked changes in chemical shifts ($\Delta\delta_{obs}$>0.15 ppm) (Fig. 3A; residues labelled yellow), suggesting an orientation in which one end of plectasin specifically is located in the membrane interface.

To identify the residues on plectasin that bind Lipid II, we then titrated plectasin bound to DPC with Lipid II. With increasing concentrations of Lipid II, another set of NMR signals appeared and became stronger, whereas the NMR signals of *apo*-plectasin bound to DPC micelles became weaker, until they disappeared at equimolar concentrations of plectasin and Lipid II, supporting the 1:1 binding stoichiometry found by TLC. Addition of extra plectasin to the mixture brought the signals of *apo*-plectasin forward again, further addition of Lipid II to equimolarity led to the disappearance of the signals again. From a 3D-HNCA spectrum we could assign backbone H^N, N and C^α signals of the plectasin:Lipid II:DPC complex . The strongest changes in chemical shift ($\Delta\delta_{obs}$>0.22 ppm) were obtained for amino acids F2, C4, D12, Y29, A31, G33, C37 and K38 (Fig. S5, Fig. S6). Most of these residues localize in a coherent patch in close proximity to the residues affected by binding to DPC (Fig. 3B, residues labelled magenta). A31, G33 and C37 exert chemical shift-changes both upon addition of DPC and Lipid II. To further verify this, site-saturated mutagenesis (where a given

amino acid is changed to each of the other 19 natural amino acids) was carried out at all positions in plectasin except the 6 cysteines. The mutant libraries were expressed in *S. cerevisiae* and 400-600 transformants of each position tested for activity against *S. aureus* in a plate overlay assay. No amino acid substitutions at positions D12, Y29 or G33 resulted in activity against *S. aureus*, whereas only the very conservative mutations of A31 to G and K38 to R resulted in activity against *S. aureus*. At other amino acid positions not involved in DPC or Lipid II binding, a wide range of non-homologous amino acid substitutions gave rise to plectasin variants retaining antimicrobial activity.

To visualize the complex between Lipid II and plectasin, docking studies using the GOLD and HADDOCK programs were performed (*15, 16*). In accordance with the NMR data, evidence in favour of a primary binding site involving the interaction of the pyro-phosphate moiety of Lipid II with the amide protons F2, G3, C4 and C37 of plectasin via hydrogen bonding was obtained (Fig. 3C). Several of the other large chemical shift changes are present in residues involved in secondary structure interactions (*e.g.* formation of beta-sheets), which most likely undergo structural changes upon binding to the target. Taken together, these data strongly support a model in which plectasin gains affinity and specificity through binding to the solvent-exposed part of Lipid II while the hydrophobic part of plectasin is located in the membrane interface. Thus, plectasin shares functional features with the lantibiotic nisin in that for both peptides the pyrophosphate moiety is most relevant for binding of Lipid II, although nisin inserts deeply into the membrane bilayer, forming pores and causing major delocalization of Lipid II (*17*,*18*).

To test whether inhibition of CW biosynthesis is restricted to plectasin or represents a general feature we tested a series of defensin peptides from other fungi, mollusc and arthropods for Lipid II binding and inhibition of the overall Lipid II synthesis and FemX reaction (Fig. S8A). Two fungal defensins, oryzeasin (from *Aspergillus oryzea*) and eurocin (*Eurotium amstelodami*) did inhibit the enzymatic reactions and bind to Lipid II in stoichiometric numbers as did the two defensins from invertebrates, lucifensin from maggots of the blowfly *Lucilia sericata* and gallicin from the mussel *Mytilus galloprovinciali* (Fig. S8BCD). In contrast, heliomicin from the tobacco budworm *Heliothis virescens* which share the conserved cysteine pattern did not show affinity for Lipid II and had no activity in these assays. These data clearly demonstrate that among the host defence peptides of eukaryotic organisms specific inhibitors of CW biosynthesis can be found which directly target Lipid II, "the bacterial Achilles' heel" for antibiotic attack (*19*).

Vancomycin, one of the very few remaining drugs for the treatment of multi-resistant gram-positive infections, has been shown to predominantly bind the D-alanyl-D-alanine (D-ala-D-ala) part of the pentapeptide in Lipid II (*11*) (Fig. 2A). However, high-level vancomycin resistance has been observed in both enterococci (VRE) and staphylococci (VRSA). Importantly, there is no cross-resistance between vancomycin and plectasin, and in contrast to vancomycin, plectasin is not competitively inhibited by the presence of the D-ala-D-ala ligand (Fig. S9). This further demonstrates that the primary interactions to Lipid II differ between plectasin and vancomycin and taken together these results suggest that future development of true cross-resistance between vancomycin and plectasin is unlikely.

Plectasin and its improved derivatives such as NZ2114 possess a range of features - such as potent activity *in vitro* under physiological conditions and in animal models of infection, low potential for unwanted toxicities, extended serum stability and *in vivo* half-life, and cost-effective large-scale manufacturing – which combined with a validated microbial target make it a promising lead for further drug development.

Reference List

1. P. H. Mygind *et al.*, *Nature* **437**, 975 (2005).
2. D. Andes, W. Craig, L. A. Nielsen, H. H. Kristensen, *Antimicrob. Agents Chemother.* **53**, 3003 (2009).
3. M. Zasloff, *Nature* **415**, 389 (2002).
4. R. E. Hancock, H. G. Sahl, *Nat. Biotechnol.* **24**, 1551 (2006).
5. B. Hutter *et al.*, *Antimicrob. Agents Chemother.* **48**, 2838 (2004).
6. F. McAleese *et al.*, *J. Bacteriol.* **188**, 1120 (2006).
7. M. Cao, T. Wang, R. Ye, J. D. Helmann, Mol. Microbiol. 45, 1267 (2002).
8. T. Mascher, N. G. Margulis, T. Wang, R. W. Ye, J. D. Helmann, Mol. Microbiol. 50, 1591 (2003).
9. H. J. van Heijenoort, *Microbiol. Mol. Biol. Rev.* **71**, 620 (2007).
10. T. Schneider *et al.*, *Mol. Microbiol.* **53**, 675 (2004).
11. P. E. Reynolds, *Eur. J. Clin. Microbiol. Infect. Dis.* **8**, 943 (1989).
12. N. E. Allen, T. I. Nicas, *FEMS Microbiol. Rev.* **26**, 511 (2003).
13. H. Brotz *et al.*, *Mol. Microbiol.* **30**, 317 (1998).
14. J. M. Willey, W. A. van der Donk, *Annu. Rev. Microbiol.* **61**, 477 (2007).
15. G. Jones, P. Willett, R. C. Glen, A. R. Leach, R. Taylor, *J. Mol. Biol.* **267**, 727 (1997).
16. C. Dominguez, R. Boelens, A. M. Bonvin, *J. Am. Chem. Soc.* **125**, 1731 (2003).
17. S. T. Hsu *et al.*, *Nat. Struct. Mol. Biol.* **11**, 963 (2004).
18. H. E. Hasper *et al.*, *Science* **313**, 1636 (2006).
19. E. Breukink, B. de Kruijff, *Nat. Rev. Drug Discov.* **5**, 321 (2006).

20. We thank Michaele Josten, Annette Hansen and Marianne R Markvardsen for expert technical assistance and acknowledge the Carlsberg Research Center for use of the 800MHz NMR spectrometer and the Obel Foundation for supporting the NMR laboratory at Aalborg University. HGS acknowledges financial support by the German Research Foundation (SA 292/10-2 and SA 292/13-1), the BMBF (SkinStaph) and by the BONFOR programme of the Medical Faculty, University of Bonn. AMJJB acknowledges financial support from the Netherlands Organization for Scientific Research (VICI grant #700.56.442). ASA acknowledges financial support from The Danish Research council for Technology and Production (274-05-0435). Competing interest statement: Allan K Nielsen, Dorothea S Raventós, Søren Neve, Birthe Ravn, Leonardo De Maria, Anders S Andersen & Hans-Henrik Kristensen are employees of Novozymes. The authors declare they have no other competing

financial interest. DNA microarray data can be accessed through ArrayExpress, accession number: E-MTAB-60. NMR assignment of ^{1}H, ^{15}N and ^{13}C atoms of plectasin have been deposited in the BioMagResBank (accession no. 16739)

Supporting Online Material

Materials and Methods

Figs S1 to S9

Tables S1 to S2

References

FIGURE LEGENDS

Fig. 1.

Effect of Plectasin on intact cells. (**A**) Classification of antimicrobial compounds using optical density measurements. Growth kinetic measurements of *B. subtilis* exposed to plectasin or various antibiotics with known cellular targets. 2-4 times the minimal inhibitory concentration (MIC) of the respective compounds were used. Plectasin (black) falls into the cluster of cell wall biosynthesis inhibiting antibiotics (red colours). (**B**) Killing kinetics of plectasin; *Staphylococcus simulans* 22 treated with plectasin at 2 × MIC (open diamonds) and 4 x MIC (squares); control without peptide (triangles). Insert shows a similar experiment with more time points within the first 60 minutes demonstrating the absence of killing in the first 30 min of treatment (**C**) Impact of plectasin on macromolecular biosynthesis in *B. subtilis* 168. Incorporation of [^{14}C]-thymidine into nucleic acids, of L-[^{14}C]-isoleucine into protein and of [^{3}H]–glucosamine in cell wall was measured in untreated controls (squares) and plectasin treated cells (open circles); glucosamine incorporation into cell wall material was selectively inhibited. (**D**) Intracellular accumulation of the ultimate soluble cell wall precursor UDP-MurNAc-pentapeptide in vancomycin-treated (dotted line) and plectasin-treated (dashed line) cells of *S. simulans* 22. Cells were treated for 30 min with plectasin or vancomycin, which is known to form a complex with Lipid II[1]. Treated cells were extracted with boiling water and the intracellular nucleotide pool analyzed by reversed HPLC. UDP-MurNAc-pentapeptide was identified by mass spectrometry using the negative mode and 1 mg/ml 6-aza-2-thiothymine (in 50% (v/v) ethanol/20 mM ammonium citrate) as matrix; the calculated monoisotopic mass is 1149.35; in addition to the singly-charged ion, the mono- and di-sodium salts are detected. (**E**) Plectasin is unable to form pores in the cytoplasmic membrane of *S. simulans* 22. Potassium efflux from living cells was monitored with a potassium-sensitive electrode. Ion leakage is expressed relative to the total amount of potassium released after addition of 1 μM of the pore forming lantibiotic nisin (100%, open diamonds). Plectasin was added at 0.2 μM (triangles) and 1 μM (open triangles); controls without peptide antibiotics (squares).

Fig. 2.

Inhibition of membrane associated cell wall biosynthesis steps. (**A**) Structure of the cell wall precursor Lipid II. (**B**) The membrane-bound steps of cell wall precursor biosynthesis and

bactoprenol ($C_{55}P$) carrier cycling in staphylococci. Cell wall biosynthesis starts in the cytoplasm with the formation of the soluble precursor UDP-MurNAc-pentapeptide (UDP-MurNAc-pp). This precursor is linked to the membrane carrier bactoprenolphosphate ($C_{55}P$) by MraY yielding Lipid I (step I). Lipid II is formed by MurG which adds *N*-acetyl-glucosamine (GlcNAc) (step II). When the interpeptide bridge, which only occurs in some Gram-positive bacteria, is accomplished (step III), the monomeric peptidoglycan unit is translocated across the cytoplasmic membrane to the outside and incorporated into the cell wall (step IV). (**C**) Inhibition of membrane associated steps of cell wall biosynthesis by plectasin. In all tests, plectasin was added in molar ratios of 0.1 to 1 with respect to the amount of the appropriate lipid substrate $C_{55}P$, Lipid I or Lipid II used in the individual test system. The amount of reaction products synthesized in the absence of plectasin was taken as 100%. Product analysis was done by thin layer chromatography (see **D**) and subsequent scintillation counting of stained and excised product-containing bands; radiolabelling was based on [^{3}H]-labelled $C_{55}P$ (for Lipid I), [^{14}C]-GlcNAc for Lipid II and [^{14}C]-glycine for Lipid II-Gly1. Error bars represents +/- SD and the experiments were repeated at least three times. Technical details on the assays, the cloning and purification of the enzymes are given in Materials and Methods. (**D**) Estimation of the stoichiometry of plectasin:Lipid II binding. Lipid II was incubated in the presence of plectasin at the molar concentration ratios indicated. The stable complex of plectasin with the Lipid II remains at the application spot whereas both components migrate to the sites indicated. At a molar ratio of 1:1 neither free Lipid II nor free plectasin were observed. Data obtained with Lipid I were comparable (not shown)**.**

Fig. 3.

NMR-based model of the plectasin/Lipid II-complex. (**A**) Surface representation of plectasin with the residues showing significant chemical shift perturbations upon binding to DPC micelles indicated in yellow. (**B**) Surface representation of plectasin with the residues showing significant chemical shift perturbations upon Lipid II titration shown in magenta. (**C**) Detailed view of the pyrophosphate binding pocket. In this proposed HADDOCK-generated model the pyrophosphate moiety forms hydrogen bonds to F2, G3, C4 and C27 and the D-γ-Glutamate of Lipid II forms a salt bridge with the N-terminus of plectasin and the side-chain of His18.

Figure 1. Effect of plectasin on intact cells

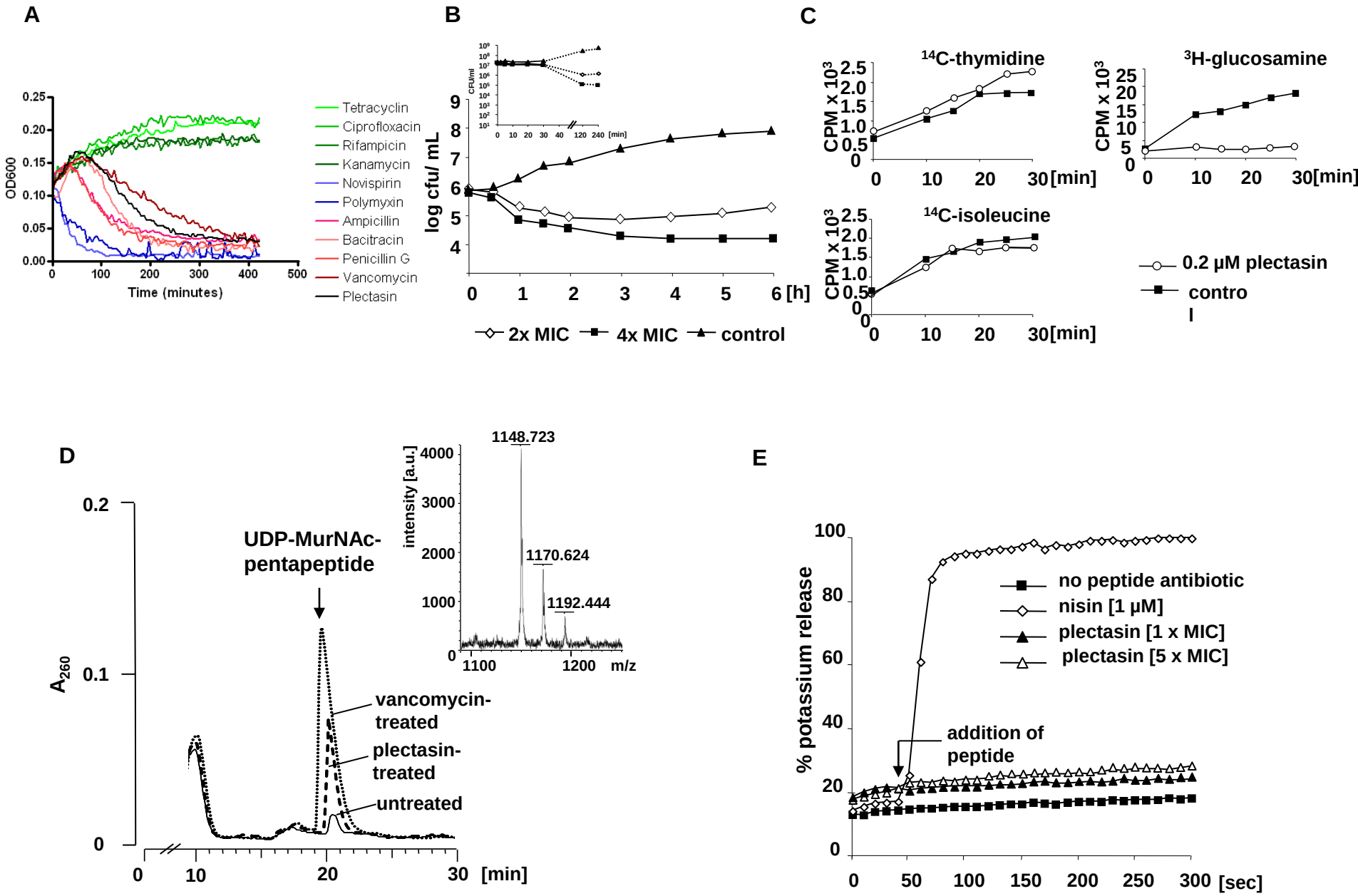

Figure 2. Inhibition of membrane associated cell wall biosynthesis steps

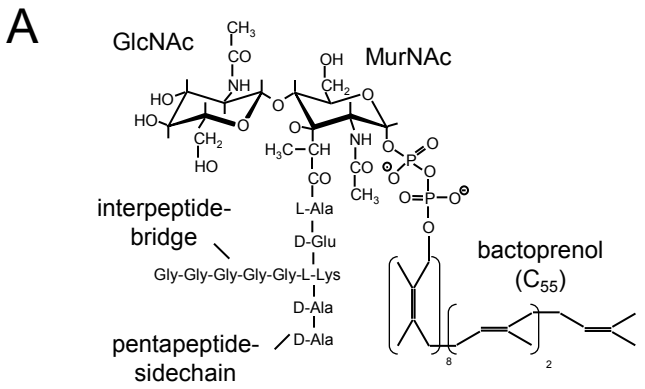

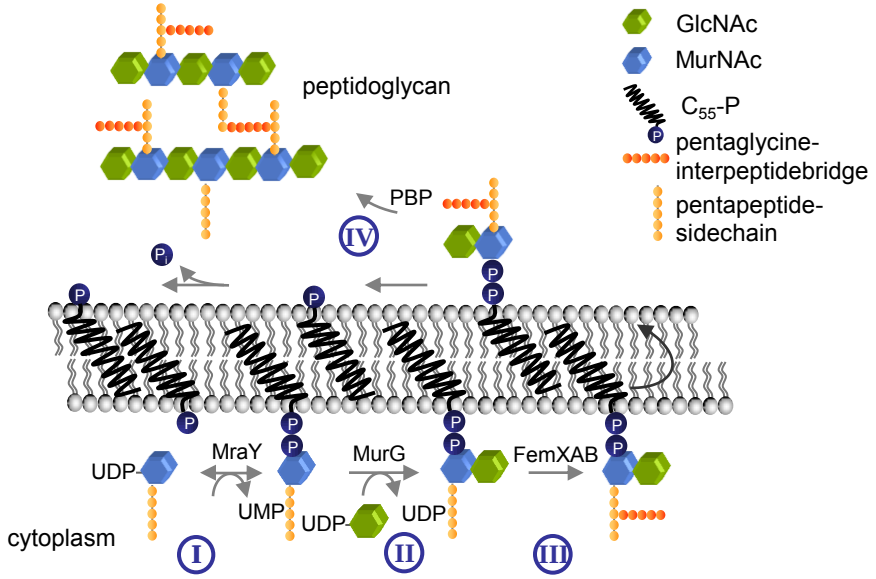

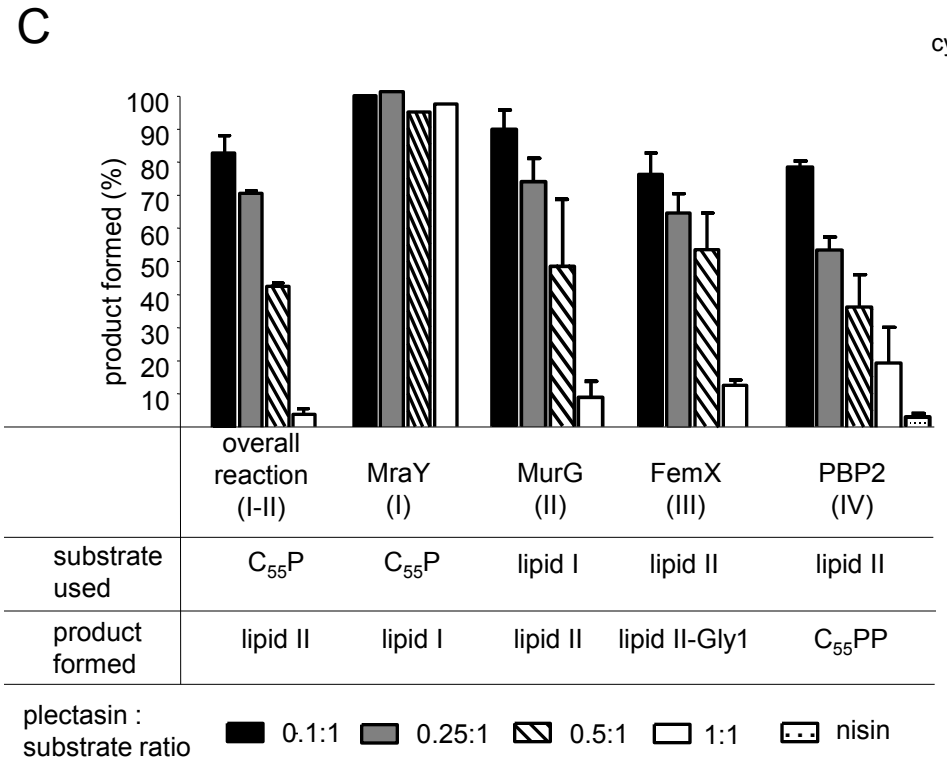

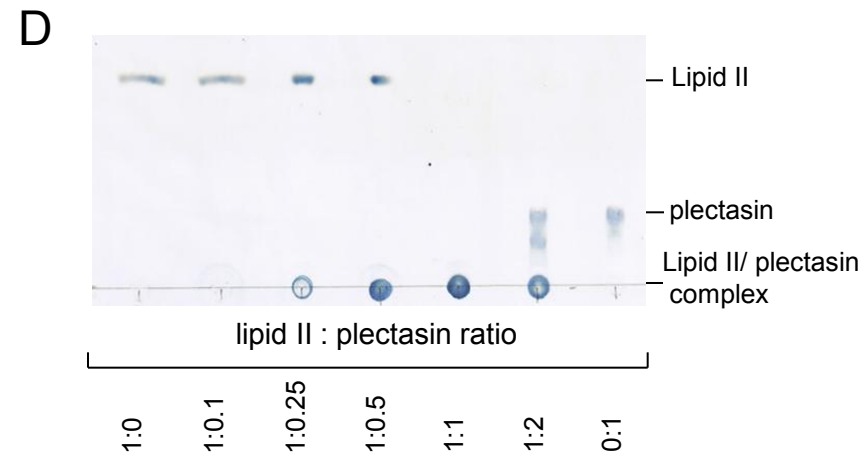

Figure 3. NMR-based model of the plectasin/Lipid II-complex